Progress in Nuclear Energy 155 (2023) 104483

Contents lists available at ScienceDirect

Progress in Nuclear Energy

journal homepage: www.elsevier.com/locate/pnucene

Statistical analysis of fuel cycle data from Swedish Pressurized Water Reactors and the impact of simplifying assumptions on simulated nuclide inventories

V. Mishra *, Zs. Elter, E. Branger, S. Grape

Division of Applied Nuclear Physics, Department of Physics & Astronomy, Uppsala University, 752 37 Uppsala, Sweden

ARTICLE INFO

Keywords:
Nuclear fuel cycle
Nuclear safeguards
Spent fuel
Sensitivity analysis
Serpent2

ABSTRACT

When analyzing and assessing properties of spent nuclear fuel (SNF) such as radionuclide inventories, the power history of the fuel during its time spent inside the reactor core plays an important role. This information can be very useful in the field of nuclear safeguards wherein a safeguards inspector can use it to verify the fuel properties such as burnup, initial enrichment and cooling time (or collectively termed as the "BIC" set of variables). However, such information may often be unavailable to the safeguards inspector or the level of detail in the available information may be lacking. Therefore, when analyzing SNF for various purposes (such as for safety, safeguards and back-end purposes), the power history of the fuel is most often disregarded altogether and the inspectors only look at the fuel BIC. If the power history-level information is considered, it is not uncommon to make simplifying assumptions about how the fuel is burned in the reactor. In this work, we perform an exploratory analysis of fuel cycle data from two PWR units of the Ringhals nuclear power plant in Sweden. The said analysis describes the variation in the number of cycles, cycle lengths, downtimes et cetera in order to develop a simplified yet representative model of irradiation that may be used to construct synthetic data libraries. Furthermore, we look into impact of changes in the power history on the nuclide inventories of key gamma emitters and isotopes responsible for decay heat in the SNF of the fuel in three different irradiation scenarios. Our results show that in most cases with fuels that are considerably long-cooled, it is acceptable and even preferred to use a simplified power history over an idealized or a representative irradiation model obtained from exploratory analysis of the fuel cycle data. However, for short-cooled fuels, using a simplified or even an idealized history is less preferable over modeling the detailed power history of the fuel due to the presence of short-lived nuclides in the SNF which are more sensitive to variations in the power history.

1. Introduction

In the domain of nuclear safeguards, accurate information detailing the reactor fuel cycle is important to model how the fuel was irradiated in the reactor. This information is also highly desirable to sectors involved in the fuel's service period as well as in the back-end. Within the service period, this information can help in proper optimization of the fuel cycle which is required for optimal fuel usage. While in the back-end, this information is used to assess spent fuel handling and storage options. To nuclear safeguards inspectors, this information is of great interest since with more accurately modeled fuel, safeguards determination of BIC (Bolind, 2014) improves the performance of prediction models for safeguards-relevant purposes. Recent interest in the use of machine learning for nuclear safeguards purposes (Bachmann et al., 2021; Grape et al., 2020; Hellesen et al., 2017; Mishra et al., 2021; Borella et al., 2017, 2019) wherein machine learning models are used to make predictions of fuel parameters has prompted the development of datasets (Rossa and Borella, 2020; Elter et al., 2020) of simulated fuel properties. These machine learning models can be trained on the radionuclide inventories of spent nuclear fuel (which can act as training input features) and can be used to deduce fuel properties like burnup (BU), initial enrichment (IE), and cooling time (CT), which are of main interest to nuclear safeguards inspectors. Since there is a lack of sufficient experimental or measurement data of SNF, these models rely on synthetic data produced using burnup simulations. This has however led to the challenge of finding a fuel type and its corresponding fuel cycle history that could be representative of a wide variety of SNF in practice.

In the present study, we aim to perform an in-depth analysis of nuclear fuel cycle data from two units of the Ringhals nuclear power plant (NPP) in Sweden to deduce insights on parameters important to

* Corresponding author.
E-mail address: vaibhav.mishra@physics.uu.se (V. Mishra).

https://doi.org/10.1016/j.pnucene.2022.104483
Received 14 April 2022; Received in revised form 13 October 2022; Accepted 23 October 2022
Available online 23 November 2022

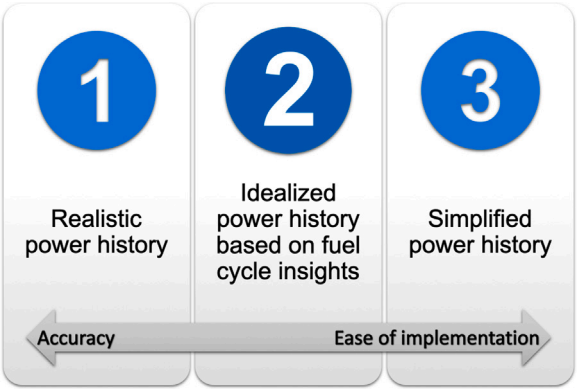

Fig. 1. Three different irradiation modeling scenarios used in Serpent2.

fuel cycle modeling. The fuel cycle data was provided by the Swedish electric corporation, Vattenfall (Anon, 2022a). The data comprised per-cycle averaged values of burnup and the corresponding downtimes for each cycle and fuel assembly. It should be noted that the actual fuel cycle data would contain additional details of burnable absorbers (like erbium or gadolinium), control rod movements and locations as well as power distributions within the core. For our analysis, such a level of detail is not required (and in practice, this information is not expected to be available for nuclear safeguards purposes). The parameters obtained from the analysis of the fuel cycle data were thereafter used for fuel burnup calculations in the Monte Carlo particle transport code, Serpent2 (Leppänen et al., 2014). The following three scenarios of fuel power history modeling were compared:

1. realistic power history: constructed using per cycle burnup data as obtained for each fuel from Vattenfall,
2. idealized power history: constructed as a representative power history based on exploratory analysis of realistic fuel cycle data from Ringhals NPP,
3. simplified power history: constructed assuming equal power at all times, and adjusting the number of cycles and final cycle length to obtain the desired burnup.

Based on this comparative assessment between the three aforementioned scenarios, we will verify whether it is more suitable to use an idealized power history of fuel burnup in place of using an oversimplified, equal averaged cycle burnup power history. In other words, this study will show if a single set of fuel cycle parameters can be used to represent all fuel from Ringhals NPP. The three scenarios have also been pictorially represented in Fig. 1.

Several studies (Bosler et al., 1982; Tomatis et al., 2017; Sweeney and Charlton, 2008) in the past have looked into estimating the impact and quantification of individual isotopic sensitivities to irradiation parameters of the SNF. However, due to the lack of availability of detailed power history data from NPPs, it is often difficult to assess whether idealization or finding a representative power history is at all feasible for modeling fuel irradiation in the core. Studies such as Mertyurek and Ilas (2022), Ilas and Liljenfeldt (2017), Ade et al. (2018) and Gauld and Mertyurek (2019) have looked into quantification of impact of modeling data assumptions on nuclide inventories in BWR SNF where the focus was more on minor actinides (MAs) and other transuranics (TRUs). Among these, Ade et al. (2018) uses power history data to assess cask reactivity for SNF from the reactor units of Forsmark NPP in Sweden while Gauld and Mertyurek (2019) provides validation of BWR SNF inventory calculation with the help of experimental data for 77 fuel samples from Japanese NPPs. There have also been attempts to use fission product signatures to fingerprint fuel by means of deducing the past power history of the fuel (Sweeney and Charlton, 2010; Grogan et al., 2018; Cheatham and Francis, 2011; Richards and Grogan, 2021; Grogan et al., 2016). Such techniques could find application in verification of fuels where the inventory could have SNF of similar BIC. Therefore, the work presented in the current study combines elements of both, the analysis of large-scale reactor power history data as well as quantification of errors introduced by variations in the modeling of fuel irradiation and thus, underscores the importance of having accurate irradiation models in modeling fuel burnup.

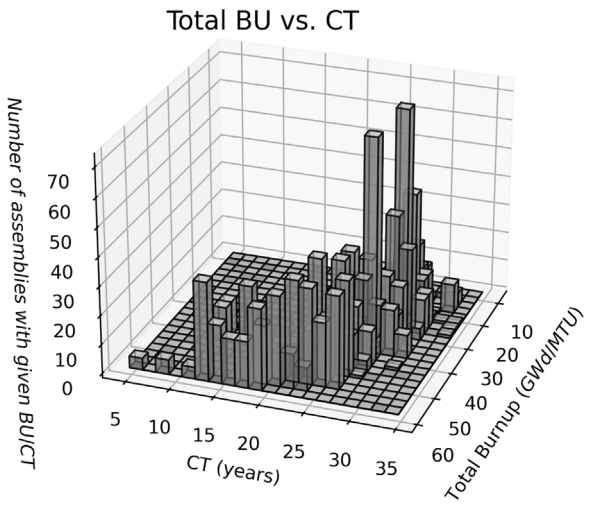

Fig. 2. Histogram of fuel properties in a BU-CT space.

2. Description of data

As mentioned previously, the fuel cycle data pertains to the Ringhals nuclear power plant which is a commercial power reactor site owned and operated by Vattenfall and Sydkraft AB. At present, the reactor site has two operating units namely, R3 and R4 (where "R" denotes Ringhals) both of which are of the Pressurized Water Reactor (PWR) type. The reactor site is located on the southern coast of Sweden about 60 km from the city of Gothenburg. The reactor unit R3 has a power rating of 1070 MWe while and R4 is rated at 1120 MWe (Anon, 2022b) and they have been in commission since the early 1980's.

The fuel cycle data comprised of detailed fuel cycle histories of a total of 2889 fuel assemblies (1501 from R3 and 1388 from R4). These fuels were used in different cycles over the decades and in summation, fuels belonged to one or more of the 33 total fuel cycles starting from the date of first operation. The total fuel inventory also included several hundred assemblies containing burnable poison in the form of gadolinium which were excluded from both the initial exploratory analysis and the later burnup calculations carried out in Serpent2. This was done since inclusion of gadolinium in the burnup calculation adds additional complexity to the fuel model due to its very high neutron absorption cross section. Furthermore, the location of the gadolinium containing fuel rods in the fuel assemblies was not available and the analysis presented in this study was based on a pincell calculation which made it difficult to include these assemblies in the analysis. Lastly, from a nuclear safeguards standpoint, it is highly uncommon that such detailed fuel information would be available to safeguards inspectors during a fuel measurement campaign. After exclusion of the gadolinium containing fuels, a total of 1448 fuels were used in the analysis, 733 from R3 and the remaining from R4. A graphical representation of the Ringhals fuel data in the BU-CT space is given in Fig. 2.

From Fig. 2 it is evident that most fuels (nearly 90%) analyzed in the present study are concentrated in the mid-high burnup region (30–60 MWd/kgU) of the histogram with only a small minority of fuels below

Table 1
Properties of fuel assemblies considered in the analysis.

	BU (MWd/kgU)	IE (wt.%)	CT (yr)
Min value	6.84	1.80	3.79
Max value	57.92	3.95	33.82
Mean value	40.65	3.34	21.41
		R3	**R4**
Fuels		733	715
LTotal		1448	

20 MWd/kgU (under 3%, which includes fuels from the fresh or the "virgin" core) showing that most fuel assemblies attained the highest achievable burnup i.e. efficient optimization of fuel cycle. Additionally, with regard to the total cooling time of the fuels considered here, more than half the fuels were over 20 years cooled and less than 1% were under 5 years cooled (valid for 2015). It should also be pointed out that the lack of fuels in the high BU-high CT region indicates that higher values of burnup eventually became achievable and most long cooled fuels show low burnup. On the enrichment end, more than 80% of the assemblies have enrichment values between 3–3.95 wt.% U-235 and less than 5% have enrichment values below 2 wt.% U-235 with the lowest enrichment being 1.8 wt.% U-235. These low enrichment fuels belonged to the first or the virgin core as they were destined for an early discharge. Therefore, there is not a significant spread in enrichment values for the fuels considered in this study. The fuel properties are also summarized in Table 1.

3. Methodology

This section provides information on the steps followed in the analysis of this paper. The first section below describes the fuel cycle parameters of interest and steps followed to extract them. The second section describes the steps followed in the burnup calculations carried out in Serpent2, the modeling assumptions and lays out the details of the fuel power history model.

3.1. Analysis of the fuel cycle

As a first step in this study, the fuel cycle data provided by Vattenfall was pre-processed to remove fuels containing gadolinium. Thereafter, individual fuel cycle data was analyzed to obtain the three key fuel cycle parameters of interest. These were: fuel cycle length, cycle downtime and the fuel burnup per cycle (BU/cycle). These parameters will later be used to set up the power history in the material burnup cases in Serpent2 for the realistic case, when this is known per assembly. The `scipy.stats` (Virtanen et al., 2020) statistics module was used in the analysis of the data. Since the complete fuel cycle data contained fuels from the first reactor fuel cycle (for both, units R3 and R4), some peculiarities in the data were expected since the first core load of fuel is often discharged without being fully burned and results in odd fuel cycle lengths and oddly low burnups. Additionally, these odd cycles likely have multiple variations in power (due to extensive testing in these phases of the reactor lifetime) and therefore the average power for such cycles is rather low. Therefore, it should be noted that in such cases, our modeled realistic history is also likely to not accurately portray the actual irradiation.

A fourth fuel cycle parameter called the fuel D–L time (discharge-to-loading time) was also looked at for fuels from units R3 and R4. This parameter was not directly used in the power history sensitivity analysis but is nevertheless an important metric that deserves attention. It is only seldom that fuels undergo contiguous (in time), uninterrupted cycles of irradiation. Apart from the scheduled cycle downtimes, this implies that fuels are often discharged from the core without attaining their terminal burnup and later reintroduced several times in the reactor. This can be done for a multitude of reasons such as cycle optimization, or in case of fuel pin leakage and failure, or in some special cases, it can also include mirror assemblies which are removed from the core when another fuel assembly fails. Such practices are not uncommon and are a part of day-to-day measures taken by operators to run the reactor in the most efficient way possible. Prolonged reactor outages can lead to long D–L times which can create problems in accurate modeling of the power history and erroneous calculation of isotopics for short-lived nuclides which might decay away during the outage time. This would not happen if the irradiation history is modeled with the same power density and time in the reactor but by disregarding the outage time between cycles.

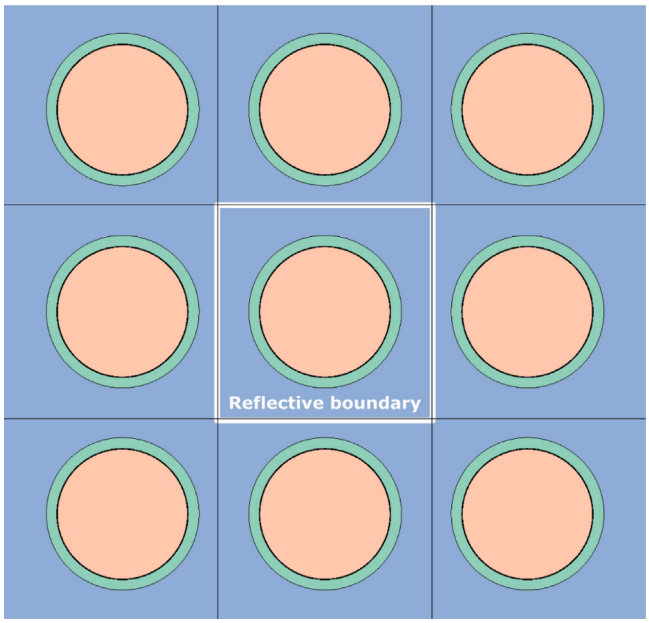

Fig. 3. A 3 × 3 unit from an infinite lattice fuel pincell model with Westinghouse 17 × 17 fuel dimensions. Orange: fuel material, green: cladding, blue: water.

3.2. Power history sensitivity analysis

Once the main parameters of interest i.e. fuel cycle length, cycle downtime and the fuel burnup per cycle (BU/cycle) were determined, they were used together in an infinite PWR pincell burnup model in Serpent2. The model was built with the design specifications of a Westinghouse 17 × 17 fuel pin (adopted from Sanders and Wagner, 2002). This assumption was made since due to control rod and fuel placement constraints, optimization leads to nearly identical physical designs for PWR 17 × 17 fuels from different manufacturers. The JEFF 3.1 (Koning et al., 2006) library was used for neutron-induced cross-section data while ENDF/B-VI (release 8) (Herman, 2009) library was used for the neutron-induced fission yields and for the decay data. A geometry plot of the 2D 3 × 3 pincell model used in the analysis is shown in Fig. 3.

Once the material burnup step in Serpent2 was complete, the radionuclide inventories were compared for three different scenarios, namely: realistic power history obtained from fuel cycle data, simplified history obtained by computing equal average cycle burnups, and lastly, with the idealized power history obtained using representative cycle burnup values obtained from fuel cycle data analysis. The fuel pin model specifications used in Serpent2 are included in Table 2.

It is important to note here that the depletion studies carried out within the scope of this analysis are conducted under the constant power setting in Serpent2. This assumption finds its basis in the fact that most commercial reactors are operated at fixed power levels with only minor power fluctuations that may occur from time-to-time for

Table 2
Fuel model specifications used in Serpent2 simulations.

Parameter	Value
Type	WE 17 × 17
Pin radius (cm)	0.4025
Clad inner radius (cm)	0.411
Clad outer radius (cm)	0.475
Fuel pitch (cm)	1.26
Fuel density (g/cm^3)	10.41
Coolant density (g/cm^3)	0.723
Coolant temperature (K)	600
Clad density (g/cm^3)	6.56
Clad material	Zircaloy
Clad temperature (K)	600
Fuel temperature (K)	900
Boron content (ppm)	630

Table 3
Primary gamma-emitting isotopes important for safeguards and their respective half-lives.
Source: Data from Bé et al. (2002)

Nuclide	Half-life	Nuclide	Half-life
^{95}Nb	34.991 d	^{95}Zr	64.032 d
^{106}Ru	371.5 d	^{134}Cs	2.064 y
^{137}Cs	30.05 y	^{141}Ce	32.5 d
^{144}Ce	284.89 d	^{154}Eu	8.601 y

economic reasons or in the case of shutdowns for planned and unplanned outages. Serpent2 offers the user to either carry out depletion at a constant power or a at constant flux. As mentioned before, constant power depletion is more applicable owing to the nature of depletion in an actual reactor core while depletion at a constant flux is better suited for conditions where irradiation conditions are to be kept unaltered as in the case of material irradiation applications where the flux from an external source is kept steady at a suitable level. A more detailed comparison of depletion under constant power versus that under constant flux is also presented in Solis et al. (2020). Additionally, the energy deposition mode selected in the Serpent2 simulations was set to its default value i.e. "`mode 0`" which denotes local deposition of fission energy at the fission sites which may produce spatially inaccurate results. The recent addition of new and more realistic energy deposition models in Serpent2 (Tuominen et al., 2019) remains to be studied in this context and can perhaps be the subject of a future study.

3.3. Nuclides of interest

The radionuclides considered for the comparative study are summarized in Table 3. The basis for selection of radionuclides listed in Table 3 lies in the fact that these isotopes are good predictors of fuel BIC and are therefore of interest from a nuclear safeguards point of view. An additional family of isotopes that were also considered in the comparative study includes isotopes listed in Table 4 as these are deemed important for determination of fuel decay heat Jansson (2002), NEA-OECD (2011). It should be pointed out that the nuclides in Table 4 are primarily responsible for decay heat after a considerable amount of time has passed since discharge from core and the fuel has cooled for at least several decades. The gamma-emitting isotopes are more short-lived, and important for safeguards verification. Therefore, they are of relevance when considering final disposal options for these fuels. At short cooling times, there are additional isotopes to consider for decay heat, although many would be included in the list of gamma nuclides as well as they are also prominent gamma emitters.

4. Results

This section describes the results from the fuel cycle analysis as well from the burnup calculations for the different fuel irradiation scenarios described in Fig. 1.

Table 4
Isotopes important for decay heat prediction used in present study and their respective half-lives.
Source: Data from Bé et al. (2002)

Nuclide	Half-life	Nuclide	Half-life
^{90}Sr	28.8 y	^{90}Y[a]	64.2 h
^{137}Ba^m[b]	2.6 min	^{238}Pu	87.7 y
^{239}Pu	24100 y	^{240}Pu	6561 y
^{241}Am	432.2 y	^{244}Cm	18.1 y

[a]Daughter of ^{90}Sr.
[b]Daughter of ^{137}Cs.

4.1. Analysis of fuel cycle data

The variation of fuel cycle length with total cycle time is shown in Fig. 4. It can be seen that for nearly all fuel cycles from both reactor units, the cycle length remains nearly the same except for a few outliers. The furthest outlier is one that is slightly longer than a 1000 days long fuel cycle for unit R3. This data point corresponds to the first cycle during which there was extensive testing and the available cycle data defines this entire period as a single cycle. The mode of the data shown in Fig. 4 is found to be 340 days. Since the mode is the most frequently appearing number in the data, it was chosen as the representative statistic for fuel cycle length. The histogram in Fig. 4 on the right side confirms these findings for both reactor units.

Similarly, the variation of cycle downtime and total cycle time is shown in Fig. 5. It is evident that the modal downtime for both units is around 24 days. As in case of fuel cycle length in Fig. 4, there are outliers present in cycle downtime data (which could be due to lengthier upgrades which resulted in longer outages), but the modal downtime can still be used as the representative downtime for these reactor units.

The distribution of fuel D–L times for both units is shown in Fig. 6. It can be seen that the modal value for the fuel D–L time is roughly 4 years. Intuitively, this value follows from the fact that the modal fuel cycle length was 340 days followed by a 24 day downtime for each cycle. Since our idealized power history comprises of four irradiation cycles, the total D–L time for the idealized power history would compute to roughly four years which is also observed to be the modal D–L value in the exploratory analysis. Therefore, the idealized power history assumes a contiguous irradiation cycles in the core instead of frequent (or infrequent) discharges of fuel and eventual re-introduction in the core to achieve the terminal burnup value. As mentioned previously in Section 4.1, unlike the other three fuel cycle parameters discussed in this section, the fuel D–L time has not been directly accounted for in the burnup cases that were set up in the following section for idealized and simplified histories. However, if the fuel D–L time is significantly long, it can have a profound impact on the radioactivity of short-lived radionuclides in the spent fuel thereby making burnup calculations differ greatly from reality. Therefore, attention must be paid to this parameter as it may be the cause of concern when dealing with models to make fuel parameter predictions.

It is important to note here that the exclusion of D–L time from the analysis presented in this study finds its basis in the fact that details of D–L time are almost never available to the safeguards inspectors. During an inspection, apart from gross defect verification, if the inspectors suspect anything, the information about fuel BIC is all that is available to the inspectors. Moreover, fuels with significantly long CT such as those used in this study (where mean CT>20 years), effects caused by longer D–L times are essentially "drowned out" as prevalence of D–L time mostly affects short-lived isotopes which have decayed away and are below the levels of detectability in such fuels.

Lastly, one of the most important parameters required for setting up the burnup calculation in Serpent2 is the burnup per cycle (or rather, the power density value for each cycle). The power density per cycle in

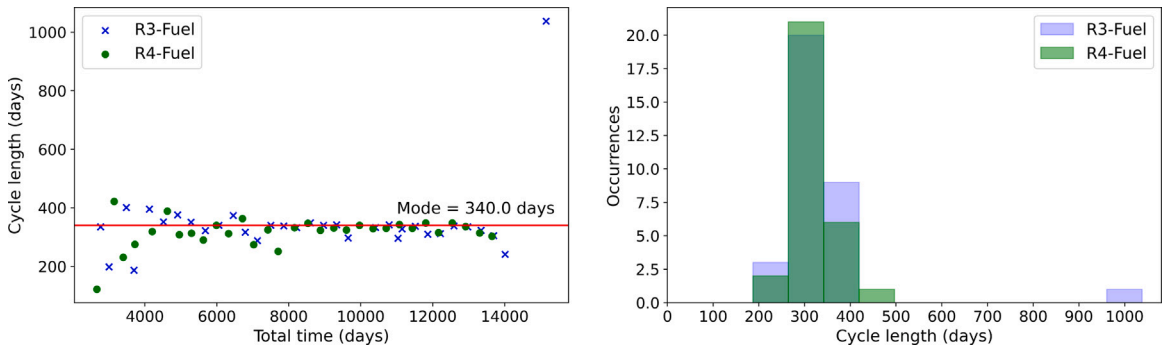

Fig. 4. Left: Fuel cycle lengths vs. total time since start of fuel cycle for R3 and R4 units. The horizontal red line indicates the location of the modal cycle length value. Right: Histogram showing the distribution of fuel cycle lengths for R3 and R4 units.

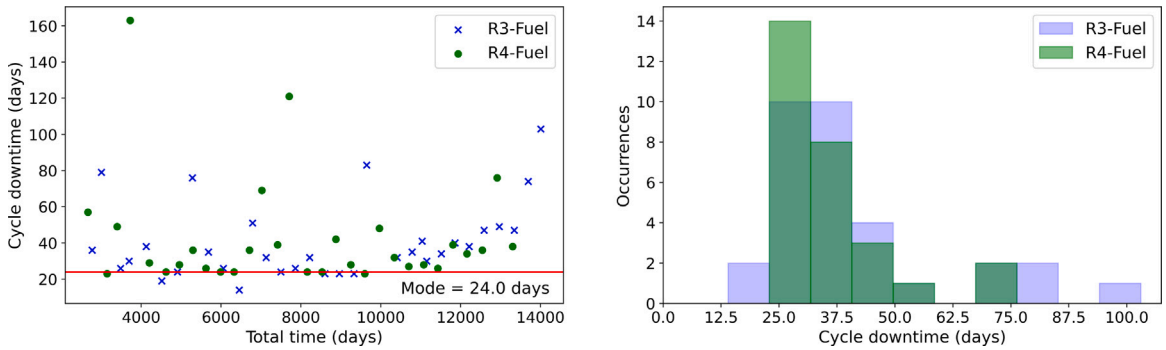

Fig. 5. Left: Fuel cycle downtime lengths vs. total time since start of fuel cycle for R3 and R4 units. The horizontal red line indicates the location of the modal cycle downtime length value. Right: Histogram showing the distribution of fuel cycle downtime lengths for R3 and R4 units.

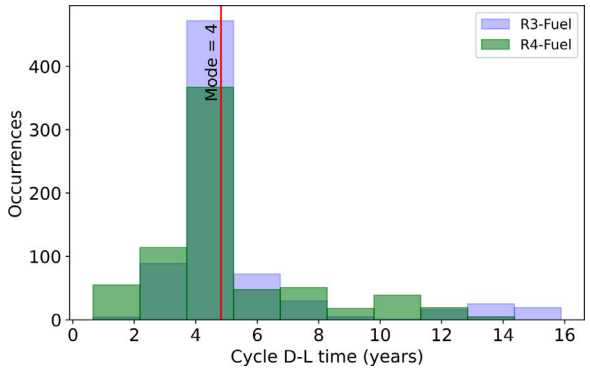

Fig. 6. Histogram showing the distribution of fuel cycle D–L times for R3 and R4 units. The vertical red line indicates the location of the modal D–L time value.

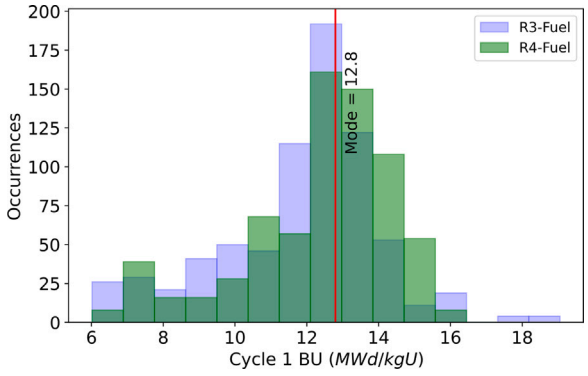

Fig. 7. Histogram showing fuel BU/cycle for the first cycle for R3 and R4 units. The vertical red line indicates the location of the modal cycle average burnup value.

Serpent2 is set using the `set powdens` card and is computed using the cycle burnup value, irradiation time and the number of irradiation steps in the cycle. For this parameter, the burnup per cycle for different fuels from R3 and R4 were assessed to obtain the representative modal value of BU/cycle for each cycle. The results for one such cycle are shown in Fig. 7. From Fig. 7 it can be inferred that the representative value for BU in the first cycle is 12.8 MWd/kgU. It is worth noting that the modal value for both, R3 and R4 units were similar. The same was repeated for all fuel cycles and it was discovered that a single representative value for BU/cycle could not be obtained for the 5th and 6th cycles due to insufficient statistics (only 4 fuels were burned long enough to have a 5th or 6th irradiation cycle). Therefore, all burnup cases assessed and reported for the idealized power history in the following section were built on the assumption that all fuels were irradiated in four cycles with limits on first three cycle and the remainder BU adjusted in the fourth cycle. The modal values for the remaining cycles are summarized in Table 5.

Table 5
Respresentative BU/cycle values for cycles 1–4 for units R3 and R4.

Cycle #	Modal BU/cycle
Cycle 1	12.8 MWd/kgU
Cycle 2	13.2 MWd/kgU
Cycle 3	11.6 MWd/kgU
Cycle 4	6.4 MWd/kgU

4.2. Power history sensitivity analysis

Once the required parameters were obtained from Section 4.1, material burnup cases corresponding to a subset of 1110 fuels from R3 and

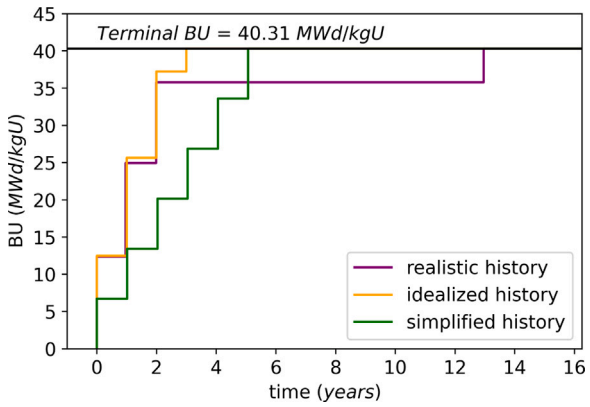

Fig. 8. A visual comparison of the three different power history scenarios for a single fuel assembly from unit R3.

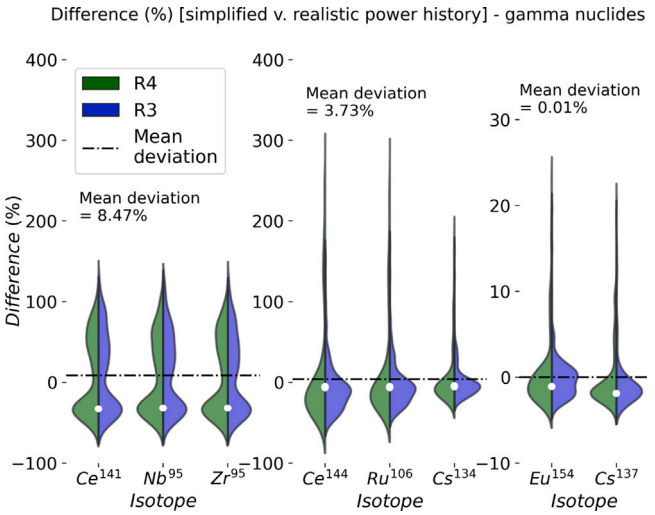

Fig. 9. Violin plots showing deviations in calculation of isotopic concentrations for R3 and R4 units between simplified power history vs. realistic power history for gamma nuclides assessed at discharge. The isotopes are grouped according to half-life.

R4 were set up. Several extremely low burnup fuels (belonging to the virgin core) as well as fuels with insufficient power history data (such as reconstituted fuels that were assembled using previously burned fuel pins) were excluded from this analysis. Additionally, the analysis also excluded fuels with burnable absorbers and fuels that acted as shielding assemblies in the past along with other fuels that were known to have grey rods (less absorbing control rods). As described previously, the sensitivity analysis was carried out with two sets of radionuclides. The first set included nuclides from Table 3 which were deemed important to gamma emissions from the spent fuel. The second includes nuclides that are primary contributors to the SNF decay heat and are listed in Table 4. The nuclides were extracted from their respective `bumat` files and no lower thresholds of any nature were considered for nuclide concentrations before further analysis. The deviations for aforementioned sets of nuclides were assessed at the time of discharge i.e. at $CT = 0$. The following sections include the results for both a simplified power history and an idealized power history when compared to the realistic power history. A visual representation of the three different scenarios of power histories for a selected fuel used in the present study is given in Fig. 8.

It can be seen clearly in Fig. 8 that the selected fuel was out of the core between its 3rd and 4th irradiation cycles (according to the realistic history) for nearly 10 years. One can observe that up to the end of the 3rd cycle (according to the realistic history), the idealized power history will better describe the realistic scenario, however due the long outage seen at the 2 year mark, the simplified history provides a better representation of the fuel's irradiation history. However, if there were no outage, clearly the idealized history best represents the realistic power history.

4.2.1. Realistic power history versus simplified power history

This first section will present the results from a comparative study between a isotopic inventories obtained from a burnup calculations carried out in Serpent2 with a realistic (detailed) power history and a simplified history with uniform average power. The results for sensitivity analysis for gamma nuclides are shown in Fig. 9. The results are reported as differences or deviations shown in the following violin plots. The difference percent, d_i is defined using nuclide number densities, c_i in Eq. (1) for each isotope i as:

$$d_i = 100 \cdot \frac{c_i^{real} - c_i^{simplified}}{c_i^{simplified}} \tag{1}$$

For the gamma nuclides from Table 3 included in Fig. 9, the deviations between the cases with a simplified power history and the realistic power history are shown as a violin plot with the global mean and median deviation (for each nuclide) values displayed as horizontal dashed line and white circle within the violin respectively. The deviations for gamma nuclides are reported separately for short-lived (like ^{95}Nb, ^{95}Zr, ^{106}Ru, ^{141}Ce and ^{144}Ce) and long-lived nuclides (^{134}Cs, ^{154}Eu and ^{137}Cs) in Fig. 9 due to differences observed in the magnitude. The plots also show the overall distribution of the deviations for all the cases assessed in the study for both units, R3 and R4. It was observed that the deviations for the two groups of short-lived nuclides such as ^{95}Nb, ^{95}Zr, ^{141}Ce, ^{144}Ce, ^{106}Ru, and ^{134}Cs were at the higher end with values reaching up to 300%. The first group consisting of ^{95}Nb, ^{95}Zr, and ^{141}Ce shows deviations of up to 150% with a mean of roughly 8% while the second group consisting of ^{144}Ce, ^{106}Ru, and ^{134}Cs showed deviations reaching 300% in case of some outliers with the mean for the three isotopes being roughly 4%. This shows that these nuclides are more sensitive to changes in the power history. It was also seen that the deviations for short-lived nuclides show a bi-modal distribution (values distributed unevenly about zero) while for the long-lived nuclides, the deviation distribution shows that calculated values for the simplified power history are consistently lower than the realistic power history. The bi-modalities arise from the fact that the realistic power histories show bi-modal distributions in the 5th and 6th cycles. These result in bi-modalities in Fig. 9 since irradiation in the final cycles is more important to estimate short-lived nuclides while the longer-lived nuclides do not exhibit the same effect.

Similarly, for nuclides important to decay heat calculations (from Table 4), the results are shown in Fig. 10.

It can be seen in Fig. 10 that compared to gamma nuclides, the global mean deviation in computation between the realistic power history and the simplified power history for the eight nuclides from Table 4 (excluding ^{134}Cs, ^{137}Cs and ^{154}Eu as they are already included in Fig. 9) is <2% while the overall median value is close to <10%. These values were lower than values obtained for gamma nuclides in Fig. 9. The primary reason for this difference between gamma and decay heat nuclides could be the fact the most nuclides responsible for decay heat in the fuel are much longer-lived than those that are responsible for gamma emissions from the SNF. The highest deviation was seen in case of ^{241}Am which has been shown in Fig. 10 on a separate canvas due to a much larger deviation seen in its numbers. This larger deviation can be understood by looking closer at its production pathway which is shown in Eqs. (2) and (3) wherein it can be seen that ^{241}Am is a nuclide that continues to form after the reactor has been shutdown or alternatively, after the fuel has been discharged (Bosler et al., 1982). From Fig. 8 it is evident that the three power history scenarios reach

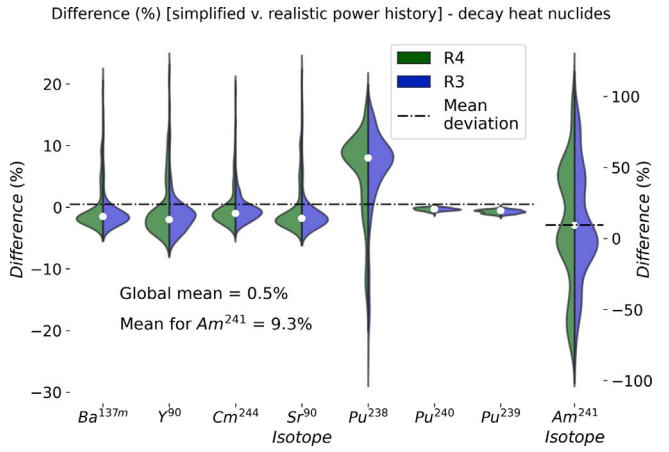

Fig. 10. Violin plots showing deviations in calculation of isotopic concentrations for R3 and R4 units between simplified power history vs. realistic power history for 8 decay heat nuclides (excluding ^{134}Cs, ^{137}Cs and ^{154}Eu) assessed at discharge.

the terminal burnups at different times. This leads to a situation where different levels of ^{241}Am buildup are estimated in realistic, simplified, and the idealized power histories of the same fuel owing to variations in the levels of ^{241}Am precursors in the production pathway. This makes ^{241}Am particularly sensitive to variations in the power history and the situation is even further exaggerated in case of fuels with long D–L times. This behavior is not seen in other isotopes since they are direct fission products (or their immediate daughter nuclei). Additionally, multi-modalities in the deviation percent are also visible similar to the short-lived nuclides from Fig. 9. This is due to sensitivity of its short-lived precursors in the SNF to variations in power history and presence of multi-modalities in the burnup for 5th and 6th cycles in the realistic power history scenario.

$$^{238}_{92}\mathrm{U} \xrightarrow{(\mathrm{n},\,\gamma)} {}^{239}_{92}\mathrm{U} \xrightarrow[23.5\ \mathrm{min}]{\beta^-} {}^{239}_{93}\mathrm{Np} \xrightarrow[2.3505\ \mathrm{d}]{\beta^-} {}^{239}_{94}\mathrm{Pu} \tag{2}$$

$$^{239}_{94}\mathrm{Pu} \xrightarrow{2(\mathrm{n},\,\gamma)} {}^{241}_{94}\mathrm{Pu} \xrightarrow[14.35\ \mathrm{yr}]{\beta^-} {}^{241}_{95}\mathrm{Am} \tag{3}$$

The isotope ^{244}Cm differs from ^{241}Am in this aspect since it follows a slightly different production pathway without long-lived precursors. The path is identical up to the formation of $^{239}_{94}$Pu as shown in Eq. (2) and then deviates slightly according to Eqs. (4) and (5) to end at $^{244}_{96}$Cm. It is therefore clear that the buildup of $^{244}_{96}$Cm is rather quick and will not show the same level of impact due to variations in power history. Lastly, as ^{137}Ba^m is the daughter of ^{137}Cs, their deviations were assumed to be identical.

$$^{239}_{94}\mathrm{Pu} \xrightarrow{4(\mathrm{n},\,\gamma)} {}^{243}_{94}\mathrm{Pu} \xrightarrow[4.956\ \mathrm{h}]{\beta^-} {}^{243}_{95}\mathrm{Am} \tag{4}$$

$$^{243}_{95}\mathrm{Am} \xrightarrow{(\mathrm{n},\,\gamma)} {}^{244}_{95}\mathrm{Am} \xrightarrow[10.1\ \mathrm{h}]{\beta^-} {}^{244}_{96}\mathrm{Cm} \tag{5}$$

4.2.2. Realistic power history versus idealized power history

This section describes the results obtained from analysis of isotopic number densities from the realistic power history and the idealized power history of the fuels. As described previously, the idealized history was obtained from the in-depth exploratory analysis of the fuel cycle data obtained from Ringhals NPP (explained further in Section 4.1). The deviations in isotopic number densities between the two scenarios are shown in Fig. 11 for gamma nuclides.

Fig. 11 shows the global mean deviation for gamma nuclides from Table 3 is roughly 9%. This was nearly 2x higher than that seen in Fig. 9 for gamma nuclides in the previous section. However, as before, the higher deviations were seen for the short-lived nuclides and the deviations were significantly lower for longer-lived ones like ^{154}Eu and

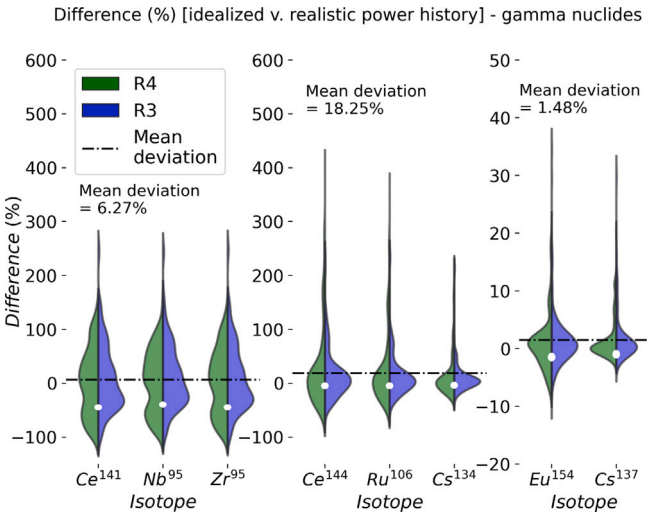

Fig. 11. Violin plots showing deviations in calculation of isotopic concentrations for R3 and R4 units between idealized power history vs. realistic power history for gamma nuclides assessed at discharge. The isotopes are grouped according to half-life.

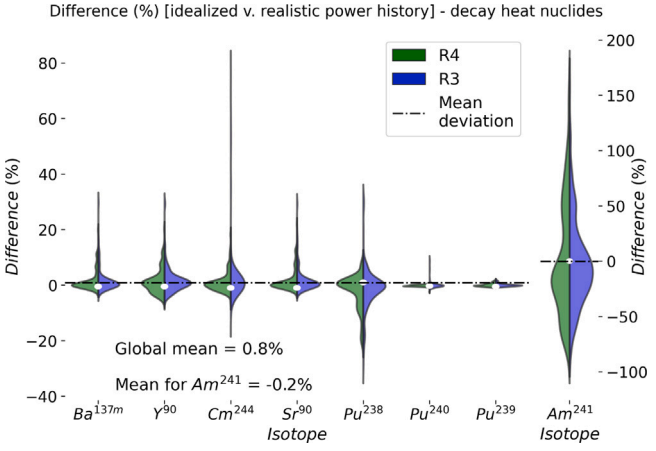

Fig. 12. Violin plots showing deviations in calculation of isotopic concentrations for R3 and R4 units between idealized power history vs. realistic power history for 8 decay heat nuclides (excluding ^{134}Cs, ^{137}Cs and ^{154}Eu) assessed at discharge.

^{137}Cs. For these long-lived nuclides, the deviations were seen to be close to 1%. For the two groups of short-lived nuclides (^{95}Nb, ^{95}Zr, ^{141}Ce, and ^{144}Ce, ^{106}Ru, ^{134}Cs), the observed deviations were between 6% and 18% respectively. As before, higher deviations for short-lived nuclides are explained best by their higher sensitivity to changes in power history, particularly in the later cycles of irradiation. Bi-modal distributions are seen again in short-lived nuclides which are explained by the bi-modal nature of burnup distributions in the 5th and 6th cycles in the realistic power history scenario.

Similarly, the deviations for decay heat nuclides from Table 4 are shown in Fig. 12. The overall behavior of deviations are similar to those observed in Fig. 10. However, it was seen that the deviations in Fig. 12 were significantly lower to those in Fig. 10 with the maximum spread in deviation values seen for isotope ^{241}Am (again shown in Fig. 12 on a separate canvas due to a much larger deviation seen in its numbers) since it is known to be more sensitive to changes in power history of the SNF. Also, one may conclude here that using a idealized history is markedly better than using a simplified history for estimating nuclides important to decay heat as deviations were nearly 3x lower. It is also worth noting that while the maximum deviation seen in the case of ^{241}Am is still on the higher side, the distribution of deviations makes

the mean much lower as compared to those seen in Fig. 10. In other words, larger deviations seen in Fig. 12 correspond to a handful of cases with abnormally high D–L times and most deviations are still concentrated in ±50%.

Therefore, it can be concluded that sensitivity towards the power history is more pronounced in the case of gamma nuclides when using an idealized history whereas, in case of decay heat nuclides, usage of an idealized power history leads to lower deviations in nuclide concentrations.

4.3. Error quantification for burnup calculations

Since Serpent2 does not compute the Monte-Carlo error for nuclide number densities on its own, an estimate of the computational deviation was obtained by generating fuel input with a different random number seeds a total of 100 times with the help of serpentTools (Johnson et al., 2020) package. Two distinct fuels with a realistic power history were chosen for this analysis, one with a more regular and contiguous (in time) power history while a second fuel had a discontinuous power history in the core. It was found that overall, the mean deviation for all nuclides of interest (both, gamma and decay heat nuclides) for both fuels was less than 1%. The highest deviation being 0.2% seen for the nuclide ^{244}Cm. Therefore it may be concluded that the deviations observed in isotopic number densities observed in Figs. 9–12 can be attributed entirely to modified power histories and not to stochastic errors in the burnup calculations.

5. Conclusions and future outlook

In the present study, we looked at the impact of using a simplified and an idealized power history in place of a realistic one to model the fuel irradiation inside the core to estimate the nuclide inventories at discharge. It was noted that the use of an idealized power history for fuels does not present any significant advantages over a simplified power history. It was found that the fuels that showed the highest deviations were those that had D–L times higher than the modal value observed in Fig. 6. These included fuels that were removed from the core after one or several cycles of irradiation and in certain cases, later re-introduced in the core to accumulate additional burnup. For some fuels, repeated removals from the core were also observed and such fuels could not be accurately represented by the idealized parameters deduced in Section 4.1. While such cases are more difficult to model and appeared to be atypical when compared to fuels with continuous cycles of irradiation and an eventual discharge from the core, such fuel loading and optimization practices are fairly common in NPPs. Therefore, as a mitigating measure, it could be worthwhile in the future work to add an offsetting parameter to the cycle downtimes to align realistic power histories with idealized ones. A number of other fuel assemblies that had high deviations belonged to a category of fuels with very low values of burnup in the last and penultimate cycles. These fuels too, could not be adequately represented by the idealized parameters. It is also important to note that for nearly all such deviant fuel assemblies, high deviations were only seen for certain short-lived nuclides (notably: ^{141}Ce, ^{95}Nb, ^{95}Zr, ^{144}Ce, ^{106}Ru and ^{134}Cs) and not others from Table 3. This could be due to the fact that these short-lived nuclides are relatively more sensitive to a fuel's power history when compared to long-lived nuclides like ^{154}Eu and ^{137}Cs. It must however be pointed out that these results hold true for assessments were made at fuel discharge. For SNF that has been cooled for several decades, the short-lived nuclides have decayed away leaving only the longest-lived nuclides behind. So, from a detectability point of view, the emissions from the short-lived nuclides are expected to fall below the lower limits of detectability of most routine safeguards verification instruments after 20–30 years of cooling leaving only the longest-lived nuclides like ^{154}Eu and ^{137}Cs behind. Therefore, our study shows that due to the complicated nature of the fuel power history, there is little to no benefit (and can often be detrimental) in using an idealized set of parameters to represent SNF's reactor power history. In that vein, it would be more appropriate to use the accurate power history in cases where such information is available or otherwise to use a simplified history involving equal cycle averaged burnups in absence of the required data. Lastly, for fuels that were excluded from the current analysis i.e. fuels with burnable absorbers like gadolinium, part length rods, grey rods etc, it must be noted that these fuels need to be verified at some point in the future. However, due to their distinctive properties, they will probably require special attention and a bespoke verification routine.

Declaration of competing interest

The authors declare that they have no known competing financial interests or personal relationships that could have appeared to influence the work reported in this paper.

Data availability

The data that has been used is confidential.

Acknowledgments

We would like to sincerely thank our collaborators, Andreas Lidén and Klaes-Håkan Bejmer at Vattenfall AB, Sweden for providing the fuel cycle data and their continued assistance during the course of the analysis presented in this study. This work has been financially supported by the Swedish Radiation Safety Authority or Strålsäkerhetsmyndigheten (SSM) under the contract SSM2017-5980.

References

Ade, B., Marshall, W., Ilas, G., et al., 2018. Impact of Operating Parameters on Extended BWR Burnup Credit, NUREG/CR-7240, ORNL/TM-2017/46. US Nuclear Regulatory Commission, Oak Ridge National Laboratory, URL https://www.nrc.gov/docs/ML1801/ML18012A191.pdf.

Anon, 2022a. Vattenfall - The Swedish State Electricity Provider's Official Webpage. URL https://www.vattenfall.se/. (Accessed 03 August 2022).

Anon, 2022b. Vattenfall.se - Ringhals AB Nuclear Site's Official Webpage. URL https://group.vattenfall.com/se/var-verksamhet/ringhals/. (Accessed: 03 August 2022).

Bachmann, A.M., Coble, J.B., Skutnik, S.E., 2021. Comparison and uncertainty of multivariate modeling techniques to characterize used nuclear fuel. Nucl. Instrum. Methods Phys. Res. A 991, 164994. http://dx.doi.org/10.1016/j.nima.2020.164994.

Bé, M.M., Helmer, R., Chisté, V., 2002. The "NUCLÉIDE" Database for Decay Data and the "International Decay Data Evaluation Project". J. Nucl. Sci. Technol. 39 (sup2), 481–484. http://dx.doi.org/10.1080/00223131.2002.10875145.

Bolind, A.M., 2014. The use of the BIC set in the characterization of used nuclear fuel assemblies by nondestructive assay. Ann. Nucl. Energy 66, 31–50. http://dx.doi.org/10.1016/j.anucene.2013.11.010.

Borella, A., Rossa, R., Turcanu, C., 2017. Signatures from the spent fuel: simulations and interpretation of the data with neural network analysis. ESARDA Bull. 55, 29–39, URL https://inis.iaea.org/search/search.aspx?orig_q=RN:49062081.

Borella, A., Rossa, R., Zaloun, H., 2019. Determination of 239Pu content in spent fuel with the SINRD technique by using artificial and natural neural networks. ESARDA Bull. 58, 41–47, URL https://publications.sckcen.be/portal/en/publications/determination-of-239pu-content-in-spent-fuel-with-the-sinrd-technique-by-using-artificial-and-natural-neural-networks(f9281fad-b0b2-4192-9e5c-11a0ce168a5f).html.

Bosler, G.E., Phillips, J.R., Wilson, W.B., et al., 1982. Production of Actinide Isotopes in Simulated PWR Fuel and Their Influence on Inherent Neutron Emission. Tech. Rep., Los Alamos National Lab., pp. 41–48, URL https://inis.iaea.org/collection/NCLCollectionStore/_Public/14/725/14725473.pdf.

Cheatham, J.R., Francis, M.W., 2011. Determining Spent Nuclear Fuel's Plutonium Content, Initial Enrichment, Burnup, and Cooling Time. Tech. Rep., Oak Ridge National Lab.(ORNL), Oak Ridge, TN (United States), URL https://www.ornl.gov/publication/determining-spent-nuclear-fuels-plutonium-content-initial-enrichment-burnup-and-cooling.

Elter, Z., Balkeståhl, L.P., Branger, E., et al., 2020. Pressurized water reactor spent nuclear fuel data library produced with the Serpent2 code. Data Brief 33, http://dx.doi.org/10.1016/j.dib.2020.106429.

Gauld, I.C., Mertyurek, U., 2019. Validation of BWR spent nuclear fuel isotopic predictions with applications to burnup credit. Nucl. Eng. Des. 345, 110–124. http://dx.doi.org/10.1016/j.nucengdes.2019.01.026.

Grape, S., Branger, E., Elter, Z., et al., 2020. Determination of spent nuclear fuel parameters using modelled signatures from non-destructive assay and random forest regression. Nucl. Instrum. Methods Phys. Res. A 969, 163979. http://dx.doi.org/10.1016/j.nima.2020.163979.

Grogan, B.R., Favalli, A., Jansson, P., et al., 2016. NDA measurement analysis of spent nuclear fuel assemblies at the Swedish clab facility using the INDEPTH code. In: INMM 57:Th Annual Meeting. URL http://urn.kb.se/resolve?urn=urn:nbn:se:uu:diva-317293.

Grogan, B.R., Purves, M., Lefebvre, J.P., 2018. Reconstructing Reactor Operating Histories Using the INDEPTH Code. Tech. Rep., Oak Ridge National Lab.(ORNL), Oak Ridge, TN (United States), URL https://www.ornl.gov/content/reconstructing-reactor-operating-histories-using-indepth-code.

Hellesen, C., Grape, S., Jansson, P., et al., 2017. Nuclear spent fuel parameter determination using multivariate analysis of fission product gamma spectra. Ann. Nucl. Energy 110, 886–895. http://dx.doi.org/10.1016/j.anucene.2017.07.035.

Herman, M., 2009. ENDF-6 Formats Manual Data Formats and Procedures for the Evaluated Nuclear Data File ENDF/B-VI and ENDF/B-VII. Tech. Rep., Brookhaven National Lab.(BNL), Upton, NY (United States)., URL https://www.bnl.gov/isd/documents/70393.pdf.

Ilas, G., Liljenfeldt, H., 2017. Decay heat uncertainty for BWR used fuel due to modeling and nuclear data uncertainties. Nucl. Eng. Des. 319, 176–184. http://dx.doi.org/10.1016/j.nucengdes.2017.05.009.

Jansson, P., 2002. Studies of Nuclear Fuel by Means of Nuclear Spectroscopic Methods, no. 714 (Ph.D. thesis). Acta Universitatis Upsaliensis, Uppsala University, Department of Nuclear and Particle Physics, p. 81, URL https://www.diva-portal.org/smash/get/diva2:116709/FULLTEXT01.pdf.

Johnson, A.E., Kotlyar, D., Terlizzi, S., et al., 2020. serpentTools: A Python package for expediting analysis with serpent. Nucl. Sci. Eng. 194 (11), 1016–1024. http://dx.doi.org/10.1080/00295639.2020.1723992.

Koning, A., Kellett, M., Mills, R., et al., 2006. JEFF Report 21: The JEFF-3.1 Nuclear Data Library. URL https://www.oecd-nea.org/dbdata/nds_jefreports/jefreport-21/jeff21.pdf.

Leppänen, J., Pusa, M., Viitanen, T., et al., 2014. The Serpent Monte Carlo code: Status, development and applications in 2013. Ann. Nucl. Energy 82, 142–150. http://dx.doi.org/10.1016/j.anucene.2014.08.024.

Mertyurek, U., Ilas, G., 2022. Nuclide inventory benchmark for BWR spent nuclear fuel: Challenges in evaluation of modeling data assumptions and uncertainties. J. Nucl. Eng. 3 (1), 18–36. http://dx.doi.org/10.3390/jne3010003.

Mishra, V., Branger, E., Elter, Z., et al., 2021. Comparison of supervised machine learning algorithms to predict PWR spent fuel parameters. In: INMM & ESARDA Joint Annual Meeting 2021. URL https://resources.inmm.org/annual-meeting-proceedings/comparison-different-supervised-machine-learning-algorithms-predict-pwr.

NEA-OECD, 2011. Spent Nuclear Fuel Assay Data for Isotopic Validation. State-of-the-Art Report, p. p23, URL https://www.oecd-nea.org/science/wpncs/ADSNF/SOAR_final.pdf.

Richards, S.M., Grogan, B.R., 2021. Sensitivity study of INDEPTH for verification of facility spent nuclear fuel declarations. Nucl. Sci. Eng. URL https://www.osti.gov/biblio/1364306-sensitivity-study-indepth-verification-facility-spent-nuclear-fuel-declarations.

Rossa, R., Borella, A., 2020. Development of the SCK CEN reference datasets for spent fuel safeguards research and development. Data Brief 30, 105462. http://dx.doi.org/10.1016/j.dib.2020.105462.

Sanders, C., Wagner, J., 2002. Study of the effect of integral burnable absorbers for PWR burnup credit. ORNL/TM-2000/321, URL https://www.nrc.gov/docs/ML0207/ML020770436.pdf.

Solis, A.H., Stankovskiy, A., Fiorito, L., et al., 2020. Depletion uncertainty analysis to the MYRRHA fuel assembly model. In: EPJ Web of Conferences, Vol. 239. EDP Sciences, p. 12001. http://dx.doi.org/10.1051/epjconf/202023912001.

Sweeney, D.J., Charlton, W.S., 2008. Physical mechanisms for fission product concentration differences from variations in reactor power history. URL https://nsspi.tamu.edu/wp-connection/upload-links/p3_pub2.pdf.

Sweeney, D.J., Charlton, W.S., 2010. Reactor Power History from Fission Product Signatures (Ph.D. thesis). Texas A & M University, URL https://nsspi.tamu.edu/reactor-power-history-from-fission-product-signatures-3266/.

Tomatis, D., Galia, A., Pastoris, S., et al., 2017. Quantification of history effects in PWR modelling. Nucl. Eng. Des. 325, 205–217. http://dx.doi.org/10.1016/j.nucengdes.2017.08.022.

Tuominen, R., Valtavirta, V., Leppänen, J., 2019. New energy deposition treatment in the Serpent 2 Monte Carlo transport code. Ann. Nucl. Energy 129, 224–232. http://dx.doi.org/10.1016/j.anucene.2019.02.003.

Virtanen, P., Gommers, R., Oliphant, T.E., et al., 2020. SciPy 1.0: Fundamental algorithms for scientific computing in pytho. Nature Methods 17, 261–272. http://dx.doi.org/10.1038/s41592-019-0686-2.